Robust registration of sparsely sectioned histology to ex-vivo MRI of temporal lobe resections

Maged Goubran[a,c], Ali R. Khan[a], Cathie Crukley[a], Susan Buchanan[a], Brendan Santyr[a], Sandrine deRibaupierre[b], Terence M. Peters[a,c]

[a]Imaging Research Laboratories, Robarts Research Institute,
[b]Department of Clinical Neurological Sciences,
[c]Department of Biomedical Engineering,

The University of Western Ontario, London, Ontario, Canada

ABSTRACT

Surgical resection of epileptic foci is a typical treatment for drug-resistant epilepsy, however, accurate pre-operative localization is challenging and often requires invasive sub-dural or intra-cranial electrode placement. The presence of cellular abnormalities in the resected tissue can be used to validate the effectiveness of multi-spectral Magnetic Resonance Imaging (MRI) in pre-operative foci localization and surgical planning. If successful, these techniques can lead to improved surgical outcomes and less invasive procedures. Towards this goal, a novel pipeline is presented here for post-operative imaging of temporal lobe specimens involving MRI and digital histology, and present and evaluate methods for bringing these images into spatial correspondence. The sparsely-sectioned histology images of resected tissue represents a challenge for 3D reconstruction which we address with a combined 3D and 2D rigid registration algorithm that alternates between slice-based and volume-based registration with the ex-vivo MRI. We also evaluate four methods for non-rigid within-plane registration using both images and fiducials, with the top performing method resulting in a target registration error of 0.87 mm. This work allows for the spatially-local comparison of histology with post-operative MRI and paves the way for eventual registration with pre-operative MRI images.

1. INTRODUCTION AND BACKGROUND

Drug-resistant epilepsy occurs in over 30% of epilepsy patients and is characterized by partial refractory seizures.[1] Temporal Lobe Epilepsy (TLE) is the most common cause of medically intractable refractory seizures, and in these cases a surgical excision of the affected brain region can be used to control seizures.[2] However, current imaging and surface EEG techniques of epileptogenic focus localization may not yield sufficient localization due to low spatial resolution, and lead to invasive electrophysiological monitoring using sub-dural strips or grid electrodes. We hypothesize that improved pre-operative localization of the focus and subsequent image-guided surgery can lead to better surgical outcomes and less invasive procedures.

To this end, we are investigating the efficacy of multi-spectral Magnetic Resonance Imaging (MRI) for localization of epileptic foci. The identification of cellular abnormalities in histological slides of the resected tissue could potentially be used as high-resolution marker to validate the effectiveness of multi-spectral magnetic resonance imaging (MRI) in pre-operative foci localization and surgical planning.[3,4] To accomplish this, spatial correspondences must be found between the histology and pre-operative MRI, however, we focus here on the first step of this problem involving the spatial correspondences between histology and ex-vivo MRI of the resected tissue. Specifically we describe the MR imaging and histological processing methods, a novel algorithm for simultaneous reconstruction and alignment of the sparsely sectioned histological data to MRI, and an evaluation of both image-based and fiducial-based methods for within-plane deformable registration between histology and MRI.

Ex-vivo imaging is an intermediate step that links digital pathology and pre-operative imaging, hence a correspondence between histology slices and ex-vivo MR images is the overall goal of this work. Furthermore, the higher resolution of specimen imaging is advantageous for examining the correlation between MRI and histology. Finding spatial correspondence is not a trivial task due to the different deformations and changes that

Medical Imaging 2012: Image Processing, edited by David R. Haynor, Sébastien Ourselin,
Proc. of SPIE Vol. 8314, 83141V · © 2012 SPIE · CCC code: 0277-786X/12/$18 · doi: 10.1117/12.911058

occur to the resected specimen during and after the surgery. Such deformations are introduced due to the physical stresses experienced during the surgery, as well as distortions to the tissue during the histological processing. A more detailed analysis of the deformations will follow in the Discussion section. The registration algorithm presented in this work accounts for the aforementioned deformations and provides a means to reconstruct digital histology for a one to one correspondence with the ex-vivo imaging.

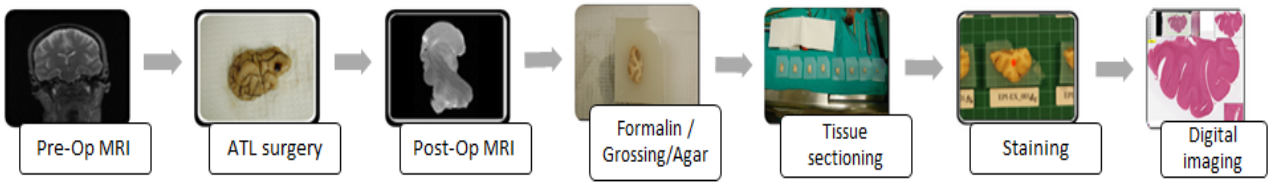

Figure 1: Overview of the acquisition and processing pipeline including pre-operative and post-operative MR imaging, histological processing, and registration of histology and MRI.

2. METHODS & MATERIALS

2.1 Patient recruitment & surgery

Temporal lobe epilepsy patients recommended for Anterior Temporal Lobectomy (ATL) - suffering from Temporal Lobe Epilepsy (TLE) and inadequate control of seizures - were recruited for the study. Prior to surgery, the patients underwent a series of 3T MRI scans including structural, diffusion-weighted imaging, and relaxation mapping, details of which are omitted since we are dealing only with post-operative data in this work. Following surgery, the resected tissue of the hippocampus and neocortex were transferred to the receiving researcher and pathology technologist for specimen imaging and histological processing. This project has been approved by the office of research and ethics of the University of Western Ontario, and informed consent has been obtained from all patients prior to their recruitment in the study.

2.2 Specimen MR imaging & histological processing

The specimens were immersed in a silicone-based lubricant 'Christo-lube' (Lubrication Technology, Inc) and imaged using a gradient-insert with a 4 channel TORO coil in a 3T MRI scanner (MR750, General Electric). Acquisitions with several different sequences were performed on the specimens including T1-weighted, T2-weighted, T1 and T2 maps. MR imaging was carried out on the specimens before and after overnight fixation in 10% formalin. T2-weighted images acquired post-fixation were used in the subsequent image processing and registration and were acquired with a balanced ssfp FIESTA sequence (TR=3.5ms, TE=1.75ms, flip angle=40°, N=4, matrix=200×200, slice thickness=0.3, FOV=60 mm).

Following MR imaging and fixation, the specimens then underwent accessioning, grossing, cut-plane identification, embedding in agar, then coronal slicing into 4.4 mm pieces. These were then processed, sectioned, stained (hematoxylin and eosin), and digitized resulting in histology images at approximately every 4.4 mm in each neocortex and hippocampus specimens.

To perform reconstruction and registration, the histology and MRI images underwent image processing that involved downsampling to 100μm and thresholding for background removal. The histology images were also median filtered and centered in a 60mm FOV frame.

2.3 3D reconstruction & alignment of histology

3D reconstruction of histology can be accomplished by aligning each slice to a reference slice (e.g. a neighbouring slice),[5,6] however, due to a sparse spacing of 4.4 mm, the anatomical features cannot be tracked from slice to slice. Utilizing reference slices in the 3D MRI can help resolve this issue, but the choice of reference slice in the MRI is non-trivial, especially if the histology sections are not enforced to be orthogonal to the MRI

acquisition plane. A combined global and local approach is proposed that alternates between 1) a global 3D image registration of the MRI volume to the histology stack to obtain reference slices, and 2) a local 2D image registration of each histology slice to each corresponding reference slice. After each iteration of these steps, the 2D rigid transformations aligning each histology section in the stack are updated and used in the following iteration until convergence. The registration used a correlation ratio cost function for the 2D and 3D rigid registration in each step with a rigid transform model (6 and 3 DOF) as implemented in the *flirt* tool[7] (FSL, `http://fsl.fmrib.ox.ac.uk/flirt`).

Algorithm 1 describes the alternating 2D and 3D registration. The input histology images, I_i^H, consisting of N slices, and the MRI volume, V^M, are given, and at each iteration k, a 3D registration between the histology stack and the MRI image is performed to generate the global rigid transformation, G^k, and 2D registrations between each corresponding slice in histology and MRI are performed to generate a local 2D rigid transformation, T_i^k.

Input: Histology images: I_i^H, $i = 1 \dots N$; MRI volume: V^M
Output: 2D transformation for aligning each histology slice: $T_i^{N_k}$; 3D transformation for aligning the MRI volume to the reconstructed histology volume: G^{N_k}
Set $T_i^0 = Id$;
for $k = 0$ *to* N_k **do**
  $V^{H^k} = \text{Stack}_{i=1\dots N}\left(I_i^H \circ T_i^k\right)$;
  $G^k = \text{argmin}_{G\in\Omega_3} C_3\left(V^{H^k}, V^M \circ G\right)$;
  for $i = 1$ *to* N **do**
    $I_i^{M^k} = \text{Slice}_i\left(V^M \circ G^k\right)$;
    $T_i^{k+1} = \text{argmin}_{T_i\in\Omega_2} C_2\left(I_i^{M^k}, I_i^H \circ T_i\right)$;
  end
end

Algorithm 1: Iterative 2D and 3D registration of the histology slices, I_i^H, and the MRI volume, V^M. The Stack and Slice functions respectively stack a set of 2D images and extract a specific slice from a volume.

2.4 Within-slice deformable registration

A deformable registration between corresponding histology and MRI slices (after above-described alignment) was employed to account for any anisotropic tissue deformations that can occur during histological processing, sectioning, and staining. Four schemes for deformable registration were evaluated for each slice:

1. **ImgReg** Fast non-rigid registration using a B-spline deformation field and a normalized mutual information cost-function[8,9] (NiftyReg,`http://sourceforge.net/projects/niftyreg/`)
2. **MaskedImgReg** The same image registration applied with an exclusion mask applied to ignore specific regions of the images during registration
3. **LmkReg** Fiducial-based non-rigid registration using Gaussian radial basis function kernels (50 cm width)[10] (PlastiMatch, `http://www.plastimatch.org`)
4. **Lmk+MaskedImgReg** The same fiducial-based non-rigid registration followed by image registration with an exclusion mask.

The B-spline image registration used a bending energy penalty weight of 10^{-3} and a three-level multi-resolution pyramid with final control point spacing of 2 mm. The binary exclusion masks were manually-defined in 3D Slicer (`http://www.slicer.org`) using a 2 mm radius paintbrush on regions of the MRI image where tissue loss is readily apparent in corresponding regions of the histology image, preventing these regions from contributing to the registration.

Fiducials were placed on the cortical gray matter boundaries with the white matter and the background, at points of extreme curvature, i.e. pits and peaks of folds. To ensure only reliable fiducial locations were used, two

different raters placed fiducials on the MRI slices with respect to a single set of histology landmarks, and where the distance between rater fiducials was greater than 1 mm fiducials were discarded.

3. RESULTS

The described methodology was carried out on the digital histology and MRI data from two subjects. The histology slices and corresponding MRI slices after 3D reconstruction and rigid alignment are shown for all slices and both subjects in Figure 1. After 3D reconstruction and rigid alignment two raters placed 110 and 75 fiducials on the histology images and corresponding MRI slices for subjects 1 and 2 respectively. After discarding fiducials where inter-rater distance was above 1mm, a total of 85 and 48 fiducials remained with a mean inter-rater distance of 0.45 mm.

Figure 2 shows the result of image-based non-rigid alignment with and without exclusion masks (MaskedImgReg) in the registration of a representative histology slice. Fiducials are shown here to aid qualitative assessment of registration accuracy and are not the same fiducials as those used for evaluation or fiducial-based registration. The non-rigid image registration is able to account for the within-plane deformations and distortions that occur in the histological processing, and the exclusion mask prevents incorrect deformations where tissue is missing in the histology. Target registration errors for each of the registration methods are summarized in Table 1, computed using one set of placed fiducials and leave-one-out cross-validation for the landmark-based registrations (LmkReg). The lowest mean TRE of 0.86/0.88 mm using exclusion-masked image-based registration is reasonable considering the resolution of 0.3 mm and mean inter-rater fiducial agreement of greater than 0.4 mm.

	Rigid	ImgReg	MaskedImgReg	LmkReg	Lmk+MaskedImgReg
Subj 1	1.00 ± 0.78	0.97 ± 0.78	0.86 ± 0.66	0.92 ± 0.69	0.88 ± 0.67
Subj 2	1.10 ± 0.90	0.97 ± 0.74	0.88 ± 0.79	1.10 ± 0.80	1.03 ± 0.87

Table 1: Target registration errors (TRE) showing the mean and standard deviation ($\mu \pm \sigma$) for each subject and registration method.

The masked image based algorithm, that accounts for tissue breakage and differential shrinkage, produced the best results among all analyzed algorithms. The image-based and masked image-based algorithms were more consistent across patients than the landmark-based algorithms, as shown by the average target registration error of all histology slices. Performing the landmark based registration before the masked image-based did not improve the accuracy of registration, however, this approach produced better result than the landmark based by itself.

4. DISCUSSION

The TRE evaluation was performed by placing fiducials on both MR and histology images for each method. The fiducials were divided into different categories according to the boundaries and folds along which they lie. Two independent raters placed fiducials on the ex-vivo MR with respect to a single set of histology landmarks. Fiducials whose placements by raters were greater than 1mm apart, were discarded to minimize the human error involved. The mean inter-rater agreement was found to be 0.45 mm. The most anterior and posterior histology slices did not contain sufficient intact tissue for reliable placement of anatomical landmarks. Acquiring more raters with a low intra rater agreement would have yielded more reliable estimates of the TRE. Other validation techniques including finding corresponding intrinsic fiducials in both histology and MRI can be performed to improve the accuracy of our validation. All the aforementioned analysis will be performed on more subjects as they are recruited in the study in order to strengthen the statistical power of these measurements.

Several challenges are met in the process of correlating MR images of resected tissue with histology. The main challenge is the deformations of the tissue encountered during the pipeline of the study. These deformations can be divided into two main categories: primary and secondary deformations. Primary deformations can be thought of as three dimensional changes such as mechanical distortions during brain extraction in the surgery, cutting in blocks or formalin fixation. Secondary deformations are within slice distortions which are due to

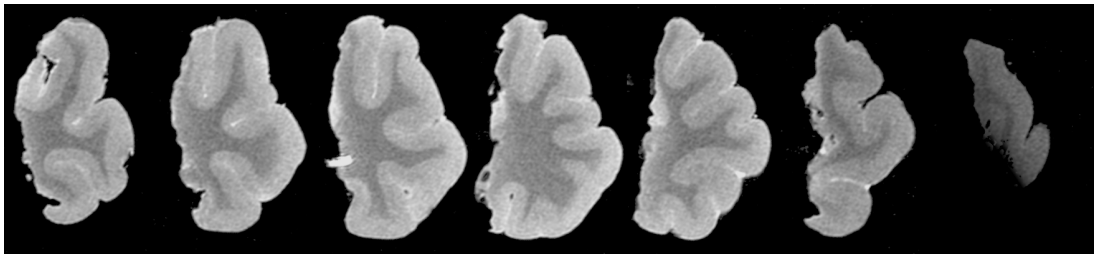

Subject 1 Rigidly-aligned MRI

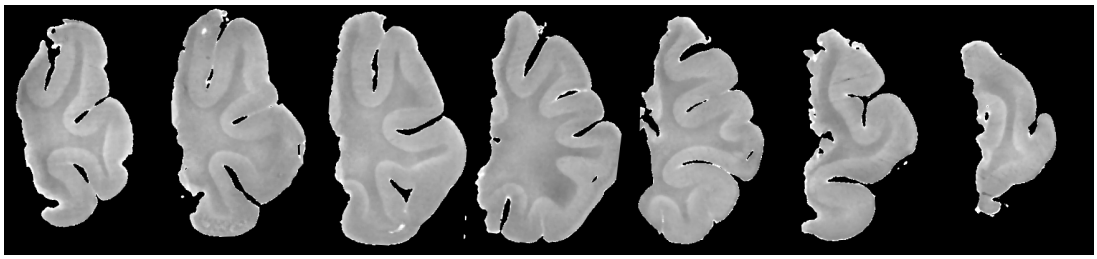

Subject 1 Rigidly-aligned Histology

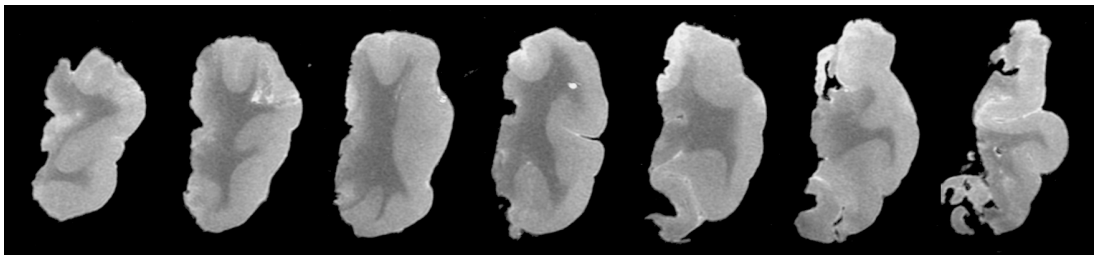

Subject 2 Rigidly-aligned MRI

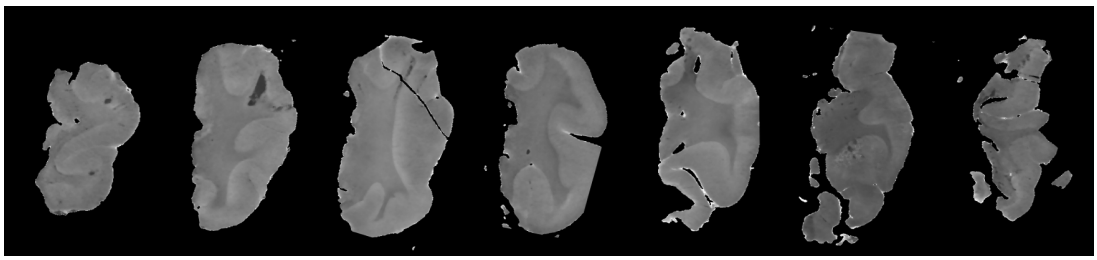

Subject 2 Rigidly-aligned Histology

Figure 2: Sequence of rigidly-aligned histology and corresponding MRI coronal slices for both subjects from anterior to posterior. Note the lack of relevant anatomic information between adjacent slices, and the breakage/loss of tissue in the most anterior and posterior histology slices. The gray appearance of histology slides is due to the image pre-processing and filtering before registration.

(a) MRI (b) Histology (c) ImageReg (d) MaskedImageReg

Figure 3: Non-rigid B-spline registration for a representative slice showing the rigidly registered MRI and histology images alongside those registered with B-spline image registration with and without an exclusion mask. Reference fiducials were placed on the MRI (red) and are displayed at the same locations in the histology slices to show alignment accuracy.

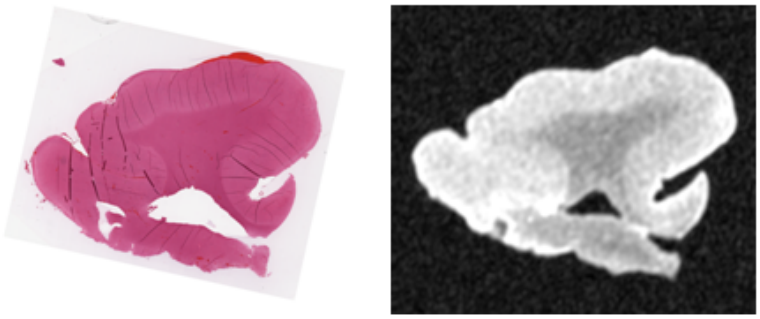

Histology slice and corresponding Ex-vivo MR slice

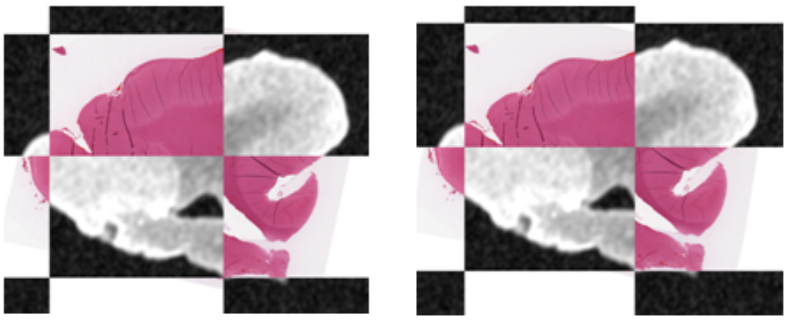

Rigidly aligned and warped slices

Figure 4: Comparison between rigid and non rigid registration showing the effect of warping on the accuracy of alignment between MR and histology.

staining or spreading histology slices over glass slides. Histology slices breakage is a major manifestation of these deformations, which motivated the use of exclusion masks in our algorithm in order to ignore the missing sections and avoid miss registration of the tissue. Moreover, differential shrinkage of the tissue is another challenge that is due to the different intrinsic properties of white and grey matter. Another significant challenge is the very different anatomy between adjacent histology slices due to the cutting at 4.4mm apart, as shown in Figure 2. The higher resolution of the specimen imaging (0.3mm) provides many opportunities to examine the physical changes and deformations that occur to the tissue after resection. One such deformation is due to the effect of formalin fixation, as well as parrafin and tissue staining, on the tissue in the processing of acquiring histology slides. The incorporation of block-face images prior to fixation may potentially alleviate this concern.

The masked imaged based algorithm outperformed the non-masked registration as expected by avoiding tissue breakage. The human error associated with placing fiducials decreased the reliability of the landmark-based algorithms, as compared to the image-based registration. This is shown in Table 1 by the fluctuation of mean TRE across the two subjects. The average target registration error of the rigid algorithm was around 1 mm, which raises the question of whether a rigid or affine algorithm might be sufficient for this type of registration. Since the ultimate goal of the study is to correlate histology slides to preoperative MR techniques, and that the resolution of our anatomical preoperative imaging is 1mm isotropic, the desired Target Registration Error for the registration algorithm is 1mm. Our validation showed that the lowest mean TRE was 0.87 mm (using masked B spline registration), which is a reasonable error considering the low number of subjects and the desired TRE.

A successful registration between histology - currently considered as the ground truth - and post-operative MRI of resected tissue is imperative for better understanding of Temporal Lobe Epilepsy at both the Micro and Macro levels. This correspondence is a key component towards achieving the overall goal of the project by bringing together information from both levels. Registering postoperative specimen imaging with digital histology paves the way for the eventual registration between preoperative MR and histology.

5. CONCLUSION

This work forms the initial stages of an ongoing project goal to correlate pre-operative MRI with digital histology. We present here a protocol for histopathological validation of multispectral Magnetic Resonance imaging of resected brain specimen, specifically temporal lobe sections. Such validation is a significant step towards epileptic foci localization for temporal lobe epilepsy. Promising results have been shown for ex-vivo MRI to histology registration on two subject datasets and we plan to investigate this further as more patients are recruited for the study.

6. ACKNOWLEDGMENTS

The authors would like to thank Dr. Seyed Mirsattari and Dr. Robert Hammond for their assistance and support throughout the study. This project is funded by the Canadian Institute of Health Research (CIHR) grant MOP 184807 and Canada Foundation for Innovation (CFI) grant 20994. MG is supported by the NSERC Create Grant CAMI award at the University of Western Ontario. AK is supported by an Epilepsy Canada postdoctoral fund.

REFERENCES

[1] Engel, J., "Etiology as a risk factor for medically refractory epilepsy: a case for early surgical intervention," *Neurology* **51**(5), 1243–4 (1998).

[2] Engel, J., Levesque, M. F., and Shields, W. D., "Surgical treatment of the epilepsies: presurgical evaluation," *Clin Neurosurg* **38**, 514–34 (1992).

[3] Eriksson, S. H., Free, S. L., Thom, M., Martinian, L., Symms, M. R., Salmenpera, T. M., McEvoy, A. W., Harkness, W., Duncan, J. S., and Sisodiya, S. M., "Correlation of quantitative MRI and neuropathology in epilepsy surgical resection specimens–T2 correlates with neuronal tissue in gray matter," *Neuroimage* **37**(1), 48–55 (2007).

[4] Howe, K. L., Dimitri, D., Heyn, C., Kiehl, T.-R., Mikulis, D., and Valiante, T., "Histologically confirmed hippocampal structural features revealed by 3T MR imaging: potential to increase diagnostic specificity of mesial temporal sclerosis," *AJNR American journal of neuroradiology* **31**(9), 1682–9 (2010).

[5] Ceritoglu, C., Wang, L., Selemon, L. D., Csernansky, J. G., Miller, M. I., and Ratnanather, J. T., "Large Deformation Diffeomorphic Metric Mapping Registration of Reconstructed 3D Histological Section Images and in vivo MR Images," *Front Hum Neurosci* **4**, 43 (2010).

[6] Chakravarty, M. M., Bertrand, G., Hodge, C. P., Sadikot, A. F., and Collins, D. L., "The creation of a brain atlas for image guided neurosurgery using serial histological data," *Neuroimage* **30**(2), 359–76 (2006).

[7] Jenkinson, M. and Smith, S., "A global optimisation method for robust affine registration of brain images," *Medical Image Analysis* **5**(2), 143–56 (2001).

[8] Rueckert, D., Sonoda, L. I., Hayes, C., Hill, D. L., Leach, M. O., and Hawkes, D. J., "Nonrigid registration using free-form deformations: application to breast MR images," *IEEE Transactions on Medical Imaging* **18**(8), 712–21 (1999).

[9] Modat, M., Ridgway, G. R., Taylor, Z. A., Lehmann, M., Barnes, J., Hawkes, D. J., Fox, N. C., and Ourselin, S., "Fast free-form deformation using graphics processing units," *Computer methods and programs in biomedicine* **98**(3), 278–84 (2010).

[10] Yuille, A. L. and Grzywacz, N. M., "A mathematical analysis of motion coherence theory," *International Journal of Computer Vision* **3**, 155–175 (1989).